Available online at www.sciencedirect.com
SCIENCE DIRECT®
Thermochimica Acta 417 (2004) 19–26
thermochimica acta
www.elsevier.com/locate/tca

Cure kinetics of a cobalt catalysed dicyanate ester monomer in air and argon atmospheres from DSC data

Iñaki Mondragon [b], Lorena Solar [a], Ileana B. Recalde [a], Clara M. Gómez [a,*]

[a] *Departament de Química Física and Institut de Ciencia dels Materials, Dr Moliner 50, Universitat de València, E-46100 Burjassot, València, Spain*
[b] *Dpto. Ing. Química y M. Ambiente, Escuela Universitat, Ingenieria T. Industrial UPV/EHU, Avd. Felipe IV 1B, 20011 San Sebatián, Spain*

Received 27 November 2003; received in revised form 27 November 2003; accepted 8 January 2004

Available online 3 March 2004

Abstract

A kinetic analysis of the cyclotrimerisation reaction of a dicyanate ester monomer catalysed by cobalt(II) acetylacetonate and nonylphenol in air and argon atmospheres has been carried out by differential scanning calorimetry (DSC). Dynamic and isothermal DSC scans as well as the glass transition temperature are the experimental data obtained. From isothermal scans a higher cyanate conversion in air than in argon was obtained. The cyanate conversions are satisfactorily described with a second-order kinetic equation in the kinetically controlled region, and by *m*-order ($m < 1$) equation after vitrification is reached. Activation energies determined by different procedures agree among them, showing slightly higher values in argon than in air.

Keywords: Cyanate ester resin; Cobalt catalyst; Kinetics; DSC

1. Introduction

Cyanate ester resins are a family of aromatic prepolymers which contain highly reactive cyanate (–OCN) functional groups [1–3]. They are currently finding widespread use in high performance aerospace and electronic applications to substitute epoxy resins in circumstances where epoxy cannot be used, such as high-temperature applications (>177 °C) [2]. The characteristic properties of cyanate resins are high thermal stability, low outgassing, radiation resistance, low dielectric constant (2.5–3.1), dimensional stability at solder temperatures ($T_g > 250$ °C) and low moisture absorption [2–5].

Due to the residual hydrogen donating impurities resulting from cyanate resin synthesis, upon heating, the cyanate groups cyclotrimerise exothermically to form triazine ring structures (Fig. 1) which result in a tightly cross linked (thermoset) structure [2,3,6–9]. For industrial purposes, the cure of these resins is achieved in presence of different catalyst systems since the cyclisation reaction is slow and usually difficult to drive to high levels of conversion, for this high curing temperatures are needed. The most common types of catalyst used for the aryl dicyanates are carboxylate salts and chelates of metal ions [2,10–12]. A co-catalyst is needed to dissolve readily the transition metal salts and chelates in molten cyanate resins [2,13].

Control of the reaction kinetics is desirable to attain good properties in the end material. Several authors have modelled the polyciclotrimerisation reaction [3,7,10,14–22]. Overall, an *n*-order autocatalytic expression has fitted non metal catalysed systems whereas a second-order rate expression was established for the metal catalysed ones. These kinetics studies do not completely agree among them. The reasons could be the different and complex catalyst systems employed, non-specification of the curing atmosphere or the technique used.

Another factor affecting the polycondensation reaction is the presence of traces of water [23,24], ideal curing conditions should include an inert atmosphere. However, in industrial conditions it is difficult, not practical, to control the curing atmosphere and both prepregs and final products are obtained without any attention paid to the atmosphere. Among the papers devoted to study the kinetics of cyanate resins, not all the papers specify the curing atmosphere and very few papers compare results in different atmospheres [7]. So, it is interesting to study the influence of the

* Corresponding author. Tel.: +34-96-354-4881; fax: +34-96-354-4564.
E-mail address: clara.gomez@uv.es (C.M. Gómez).

0040-6031/$ – see front matter © 2004 Elsevier B.V. All rights reserved.
doi:10.1016/j.tca.2004.01.011

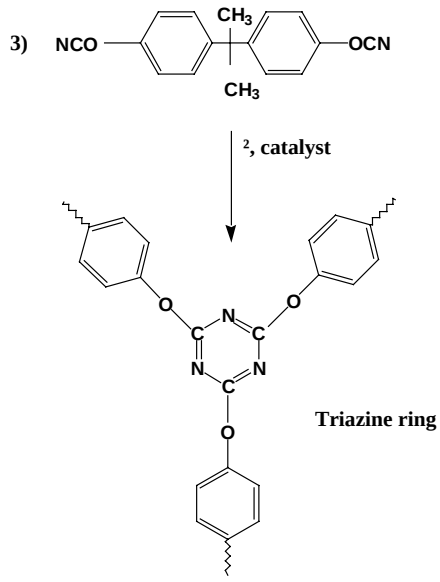

Fig. 1. Polycyclotrimerisation reaction of bisphenol A dicyanate to form triazine rings.

atmosphere in the kinetics of catalysed cyanate resins. Among all the techniques used for this purpose, differential scanning calorimetry (DSC) seems a convenient tool since it monitors the reaction during the entire range of cure and allows an accurate control of the curing atmosphere [25]. The basic assumption made in treating calorimetric data to obtain reaction kinetics is that the heat of reaction evolved at any time is proportional to the number of moles of reactant consumed. Moreover, it is also assumed that the specific heat of the material either stays constant or varies linearly with scanning temperature during a scan while both the temperature and degree of cure change simultaneously.

This paper is aimed to study the kinetics of a catalysed dicyanate ester monomer in air and argon atmospheres by DSC. The well-known bisphenol A dicyanate, Arocy B10 cured in the presence of cobalt(II) acetylacetonate catalyst, and nonylphenol as co-catalyst has been investigated. From dynamic and isothermal DSC experiments empirical rate expressions and activation energies have been deduced.

2. Experimental

2.1. Materials and sample preparation

A bisphenol A-based cyanate resin, BADCy (4,4′-dicyanato-2,2′-diphenylpropane) monomer with the trade name AroCy B10, 99.5% purity and with a cyanate equivalent of 139 g eq.$^{-1}$, was gently supplied by Ciba-Geigy. The catalyst system formed by the complex metal cobalt(II) acetylacetonate, $Co(AcAc)_2$, and the co-catalyst nonylphenol, NP, (technical grade) were obtained from Aldrich.

Cyanate resins were blended with the required amount of the catalytic system $Co(AcAc)_2$ at 360 ppm and NP at 2% of the total resin weight, prior to cure. The required amount of metal catalyst was predisolved in NP at 100 °C with continuous stirring until an homogeneous mixture was obtained and cooled down to room temperature. The catalytic blend was added to the preselected weight of the molten cyanate resin at 90 °C, stirred for 5 min to obtain an homogeneous mixture and immediately quenched before any reaction could occur. Prior to cure, the catalysed samples were stored in the refrigerator in a desiccator to avoid moisture absorption.

2.2. Conversion characterisation

Differential scanning calorimetry measurements were performed with a Perkin-Elmer DSC7 supported by a Perkin-Elmer computer running DSC7 software kit (version 3.1) for data acquisition. The DSC was calibrated with high purity indium and zinc in fully dry air and argon atmospheres. A sample mass of 8–10 mg was selected as a compromise between the thermal detection limit and the existence of thermal gradients in the sample. The DSC aluminium pans were sealed with holed aluminium lids and experiments were conducted under an air or argon atmospheres at a flow of 20 ml min^{-1}. Dynamic scans were carried out from 40 to 400 °C at different heating rates from 5 to 25 °C min^{-1}. Isothermal curing was carried out at six curing temperatures (T_c = 130, 140, 150, 160, 170, and 190 °C), after these experiments the samples were quenched to room temperature. All the samples were then subjected to a dynamic DSC scan from 30 to 380 °C at 10 °C min^{-1} to determine the residual heat of reaction, ΔH_{res}, and the glass transition temperature, T_g, of the cured material. In a third dynamic scan, the T_g of the fully cured material, $T_{g\infty}$, was determined. The temperature corresponding to the midpoint of the transition was taken as the T_g, and the residual heat of reaction was calculated from the exothermic peak by integrating the area between the heat flow curve and the base line. The conversion of each sample under isothermal conditions by assuming a single reaction mechanism can be calculated by:

$$\alpha = \frac{(\Delta H_{iso})_t}{\Delta H_{iso} + \Delta H_{res}} \quad (1)$$

where $(\Delta H_{iso})_t$ is the heat of reaction at a time t calculated from the isothermal mode, and $(\Delta H_{iso} + \Delta H_{res})$ the total heat of reaction obtained from the addition of the total heat from the isothermal mode, ΔH_{iso}, to the residual one. The accuracy of the values $(\Delta H_{iso} + \Delta H_{res})$ is ±10 J g^{-1} with respect the polymerisation enthalpies, ΔH_{tot}, calculated from dynamic scans at 10 °C min^{-1} (ΔH_{tot} = 710 ± 10 J g^{-1}). These values are in agreement with literature data [1–5].

3. Results and discussion

In order to determine the kinetic parameters: the *n*-order, the kinetic constant and activation energy, E_a, for the

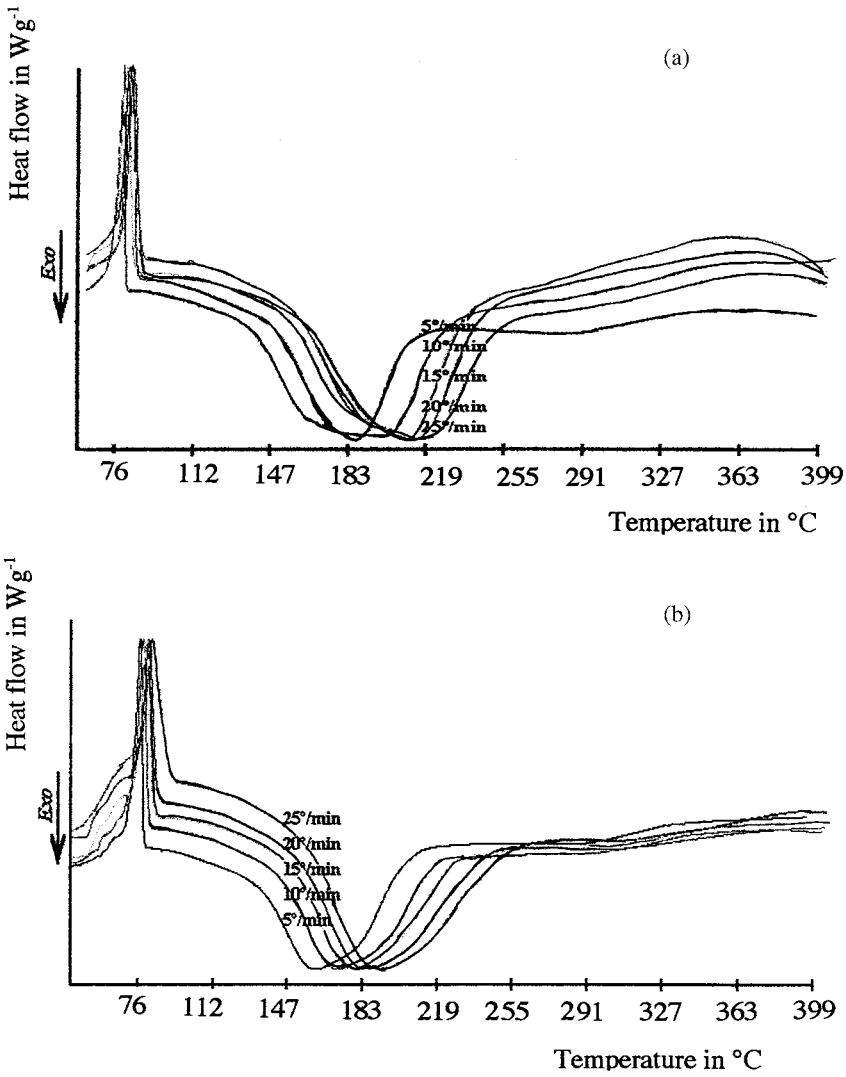

Fig. 2. Dynamic DSC scans at different heating rates in: (a) air atmosphere, and (b) argon atmosphere.

polycyclotrimerisation reaction of cobalt catalysed Arocy B10 in air and in argon, we have employed dynamic (multi-heating) and isothermal methods.

Fig. 2 shows the DSC dynamic scans of catalysed Arocy B10 at five heating rates ($\phi = 5$, 10, 15, 20 and 25 $^\circ$ min^{-1}) in both atmospheres, air (part a) and argon (part b). A sharp melting endotherm (around 80 °C) followed by an exotherm peak representing the progression of polycyclotrimerisation is observed, being this peak broader in air. Similar DSC behaviour was found for the freshly prepared samples indicating that the storage procedure does not alter the characteristic features of the uncured system (not shown for simplicity). The similarity of the heats of reaction for the two systems indicates that similar reactions occur for both of them. As the heating rate increases, values of the peak temperature, T_p, shift towards higher temperatures and are higher in air ($T_p = 194\,^\circ$C at $\phi = 10\,^\circ$ min^{-1}) than in argon ($T_p = 173\,^\circ$C at $\phi = 10\,^\circ$ min^{-1}) indicating, in principle, less reactivity in air. It was also found a slight increase of the relative area of the shoulder preceding the main exothermic peak at its expenses. The main reaction exotherms show a preceding (in air) or succeeding (in argon) shoulder and they are followed by a low shoulder (100 °C wide). The former is an indication for the presence of parallel reaction mechanisms [17,26,27]. The 100 °C wide shoulder at the high-temperature side is related to vitrification and diffusion-controlled cure as deduced from temperature modulated DSC [15]. These results are also in good agreement with those found by Barton et al. [27] with a copper(II) naphthenate catalyst and by Harismendy et al. [28] with a copper(II) acetylacetonate catalyst.

The rate of kinetically controlled reaction may be expressed by an equation of the type:

$$\frac{d\alpha}{dt} = k\, f(\alpha) = A\, f(\alpha) \exp\left(\frac{-E_a}{RT}\right) \quad (2)$$

where A is a pre-exponential factor, T the cure temperature, $k = A\exp(-E_a/RT)$ the Arrhenius rate constant, and $f(\alpha)$

is assumed to be a function of conversion independent of temperature. In terms of the heating rate, $\phi = dT/dt$, Eq. (2) can be written as:

$$\frac{d\alpha}{dT} = \frac{A}{\phi}\exp\left(-\frac{E_a}{RT}\right) f(\alpha) \quad (3)$$

From this expression a common multi-heating method to determine E_a was deduced by Ozawa [29] obtaining a simple relationship [30] at a certain degree of conversion between the heating rate, ϕ, and the temperature. So, by rearranging this expression, integrating and applying logarithms it yields:

$$\ln\int_0^{\alpha_i}\frac{d\alpha}{f(\alpha)} = \ln\frac{A}{\phi} + \ln\int_0^{T}\exp\left(-\frac{E_a}{RT}\right)dT \quad (4)$$

by assuming that ϕ is constant.

Doyle [31] defined the polynomic function:

$$P\left(\frac{E_a}{RT}\right) = \frac{R}{E_a}\int_0^{T}\exp\left(-\frac{E_a}{RT}\right)dT \quad (5)$$

that for values $20 < E_a/RT < 60$ can be substituted by:

$$\ln P\left(\frac{E_a}{RT}\right) = -5.330 - 1.0516\frac{E_a}{RT} \quad (6)$$

then, by equalling the logarithmic form of Eq. (5) to Eq. (6) and substituting in Eq. (4) it yields:

$$\ln\int_0^{\alpha}\frac{d\alpha}{f(\alpha)} = \ln\frac{A}{\phi} - 5.330 - \ln\frac{R}{E_a} - 1.0516\frac{E_a}{RT} \quad (7)$$

the left hand side is constant at a certain conversion degree and the following relation can be attained:

$$\ln\phi = Z - 1.0516\frac{E_a}{RT} \quad (8)$$

Z being a constant that depends on the collision factor, on the concentration dependent part of the rate expression, $f(\alpha)$, and on the apparent activation energy, E_a. For thermoset curing, the extent of the reaction at the exothermic peak can be considered as constant and independent of the heating rate, although the temperature at which the exothermic peak, T_p, occurs depends on the heating rate [32]. The activation energy can be calculated from a plot of $\ln\phi$ versus $1/T_p$, as shown in Fig. 3, from several DSC curves. These plots are linear ($r > 0.999$) and seed values of $E_a = 82.6\,kJ\,mol^{-1}$, $Z = 22.4$ in air, and $E_a = 91.8\,kJ\,mol^{-1}$, $Z = 25.6$ in argon. These values are in good agreement those reported in the literature [1–5]

The kinetic of a dicyanate ester monomer, Arocy B10, has also been studied by differential scanning calorimetry at different isothermal temperatures ranging from 130 to 190 °C. DSC which measures the heat flow from the reacting system has been reported to be a reliable technique to monitor the overall kinetics of thermosets [25]. The thermal polymerisation of a cyanate ester is a complex process involving large changes in viscosity and changes of state. For these reasons the kinetics derived from DSC must be treated as

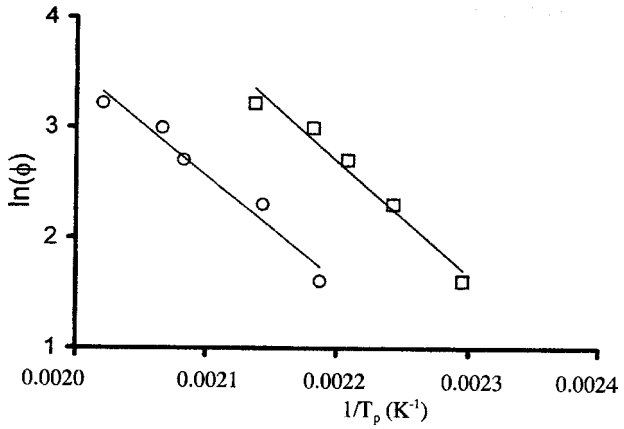

Fig. 3. Plot of ln(heating rate), $\ln\phi$, against 1/(peak temperature), $1/T_p$ in air (○) and argon (□) atmospheres.

a phenomenological analysis. A practical problem that requires the knowledge of the overall kinetics is predicting the progress of cure at different temperatures. Obviously, DSC data do not allow the measured heat flow to be separated into contributions from single reactions.

ArocyB10 resin exhibits bell-shaped exotherms (figures not shown for simplicity) corresponding to the catalysed polycyclotrimerisation reaction in air and argon atmospheres for 4 h at constant temperature (from 130 to 190 °C). These curves allow to determine the cyanate conversion as a function of time at every curing temperature from Eq. (1). Fig. 4 shows values of the cyanate conversion, α, so obtained as a function of the cure time, t, at the different curing temperatures, T, for cobalt catalysed Arocy B10 in air (part a) and argon (part b) atmospheres. Values of $T_g > T$ have been found after 4 h curing at $T > 150$ °C in air and $T > 190$ °C in argon atmospheres which indicate that these systems have vitrified (see Table 1). After the second dynamic scan the glass transition temperature of the fully reacted resin was 298 ± 2°C. The rate of dicyanate conversion is initially rapid above 140 °C curing temperature and then slows down, reaching a plateau conversion, α_p. The end of the kinetic controlled regime (the reaction is not longer controlled by the temperature and the concentration of reactive species), and the beginning of the diffusion regime (the reaction becomes dominated by mass transfer) was dependent on the curing temperature. Most of the papers dealing with thermosets systems invoke to a change from chemical-controlled kinetics to diffusion-controlled kinetics after gelation. Higher curing temperature is needed in argon atmosphere than in air to reach total cyanate groups conversion according to Fig. 4.

Time-temperature shifts of α versus ln(time) data at different cure temperatures yield a master curve for the reaction at an arbitrary selected reference temperature, T_r. The theoretical basis for the superposition is the assumption that the function that represents the variation of conversion with time, $f(\alpha)$, is independent of the temperature and that the polymerisation is kinetically controlled with a single activation energy which is assumed to be that of the overall

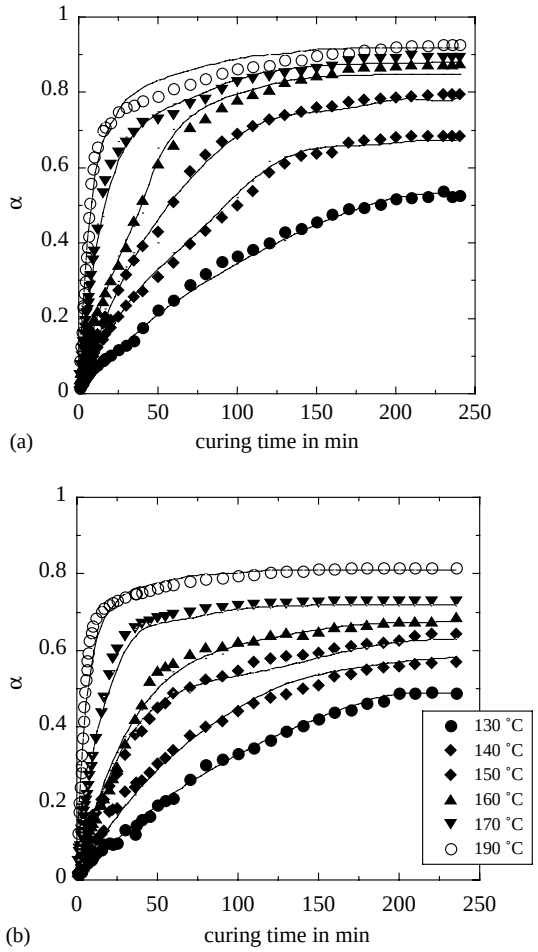

Fig. 4. Cyanate conversion as a function of curing time and curing temperature in: (a) air atmosphere, and (b) argon atmosphere. The solid line is the best fit of the data to Eqs. (11a) and (11b).

reaction [33]. Rearranging Eq. (2) and integrating, a shift factor, a_T, is defined as:

$$a_T = \ln t_r - \ln t = \left(\frac{-E_a}{R}\right)\left(\frac{1}{T} - \frac{1}{T_r}\right) \quad (9)$$

where t_r is a reference time such as the conversion degree attained at a certain T_r equal to that obtained for a T at a time t [33–35].

Table 1
Cyanate conversion, α, and glass transition temperature, T_g, for different curing temperatures in air and argon atmospheres

Air			Argon	
T (°C)	α	T_g	α	T_g
130	0.53	82	0.49	70
140	0.68	132	0.57	95
150	0.79	178	0.64	119
160	0.87	218	0.68	133
170	0.89	227	0.73	150
190	0.93	254	0.82	193

The conversions overlay at $T_r = 150\,°C$ indicate that below ≅50% conversion the experimental data for all the temperatures form a single curve while above 50% the curve starts to diverge and the cyanate conversion increases as the temperature does. Consequently, below 50% conversion, the effect of diffusion on the kinetics is not evident and the reaction is kinetically controlled, but above 50% conversion the cure kinetics becomes increasingly diffusion limited. It was observed in our experiments and also indicated by Simon et al. [36] that the onset of diffusion control occurred well before vitrification. The excellent superimposition of α versus ln(time) curves (figure not shown) until approximately 50% conversion confirms that the network structure is determined exclusively by the conversion level attained in the polymerisation, independently of the selected cure temperature. Plotting the shift factors as a function of $1/T$ (K^{-1}) allows to obtain the activation energy of the polymerisation from the slope with values of $E_a = 85.2\,kJ\,mol^{-1}$ in air, and $E_a = 90.7\,kJ\,mol^{-1}$ in argon.

Isoconversional kinetic analysis also offers a viable alternative of determining the activation energy at a certain degree of conversion without knowing any explicit kinetic model nor its parameters. The basic idea of this type of analysis is that the reaction rate at a constant conversion depends only on the temperature. In other words, Eq. (2) can be written in a logarithmic form for a certain α conversion as:

$$\ln(d\alpha/dt)_\alpha = \ln[A\ f(\alpha)] - \frac{E_{a,\alpha}}{RT} \quad (10)$$

where $E_{a,\alpha}$ should be the effective activation energy at a given conversion. For a single-step process, $E_{a,\alpha}$ is independent of α and may have the meaning of the intrinsic activation energy. Multistep processes reveal the dependence of $E_{a,\alpha}$ on α, the analysis of which helps not only to disclose the complexity of a process but also to identify its kinetic scheme [37]. We determine $d\alpha/dt$ data from Fig. 4 for each curing temperature having this function a maximum around 0.1 conversion. The plots of $d\alpha/dt$ versus α (not shown) quickly decrease in the initial times of reaction until $\alpha = 0.20$–0.40, then $d\alpha/dt$ shows a small dependence on α. After $\alpha \approx 0.55$–0.60 diffusion control slow down the reaction leading, close the end of the reaction, to a faster decrease in reaction rate. From this conversion the intensive cross-linking reaction has occurred then reducing molecular mobility, and the curing reaction changes from a kinetic to a diffusion-controlled regime. At first sight we think that this is not an autocatalytic process since the maximum conversion rate occurs at $\alpha = 0.1$ and for the autocatalytic reactions, in most thermosets, it should appear at $\alpha = 0.2$–0.4 [10,30,38]. However, Leroy et al. [15] found for a similar cyanate resin (LECY) that the autocatalytic term is not negligible even if the reaction is catalyzed. For a given α value, $\ln(A\,f(\alpha))$ is constant by assuming that the functionality $f(\alpha)$ is independent of temperature. The plot of $\ln(d\alpha/dt)_\alpha$ versus $1/T$ at each α gives a straight line from which slope the activation energy at a certain degree of conversion can

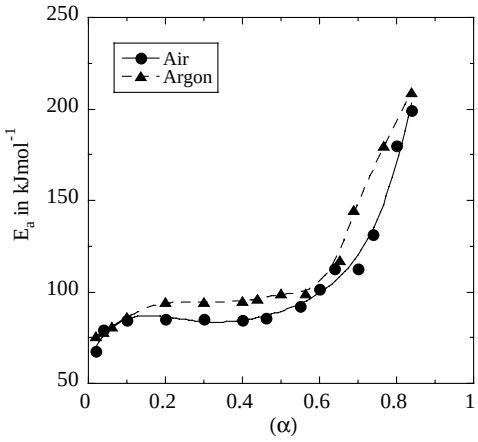

Fig. 5. Dependence of the activation energy upon conversion obtained from Eq. (10) in air and argon atmospheres.

be obtained. These activation energies values are plotted in Fig. 5 as a function of conversion. At$\alpha < 0.1$–0.2, E_a slowly increases to reach a plateau or constant with mean value $E_a = 84.7\,\mathrm{kJ\,mol^{-1}}$ in air and $94.8\,\mathrm{kJ\,mol^{-1}}$ in argon from $\alpha = 0.2$–0.60, for higher α values ($\alpha > 0.6$) an increase is noticed, probably due to the medium viscosity increase. Changes in E_a are due to changes in the mean average size of the molecules, in the cross-linking degree and in the reactivity of the different species. The values of E_a as a function of conversion show an almost constant value, deviating from this at very low or very high conversions, similarly to data found for the cure of epoxy systems [16,37,39]. The values of E_a in air are lower than in argon [7] and the plateau or mean E_a values are very similar to those obtained by the other procedures used in this paper. So, it is a good approximation to assume that E_a is a constant between a conversion of 0.20 and 0.60.

Now, we will use a phenomenological kinetic analysis based on the simple *n*th-order model with respect to the cyanate as measured by the disappearance of cyanate groups to analyse kinetic data. To this end, we clearly define two conversion regions:

$$\frac{d\alpha}{dt} = k(1-\alpha)^n, \quad \alpha<\alpha_d \tag{11a}$$

$$\frac{d\alpha}{dt} = k_d(\alpha_p-\alpha)^m, \quad \alpha \geq \alpha_d \tag{11b}$$

where α_p is the plateau conversion, α_d the onset of diffusion control, n and m the reaction kinetic exponents, and k and k_d are the corresponding rate constants.

The kinetically controlled conversion range ($\alpha < \alpha_d$) was successfully fitted assuming a second-order reaction, $n = 2$, in Eq. (11a). All the kinetic data analysed (Fig. 4) give good linear fits ($r > 0.999$) by plotting $1/(1-\alpha)$ versus curing time at every temperature, being higher in air than in argon, from which slope the rate constants are obtained. These k values show an Arrhenius dependence with temperature

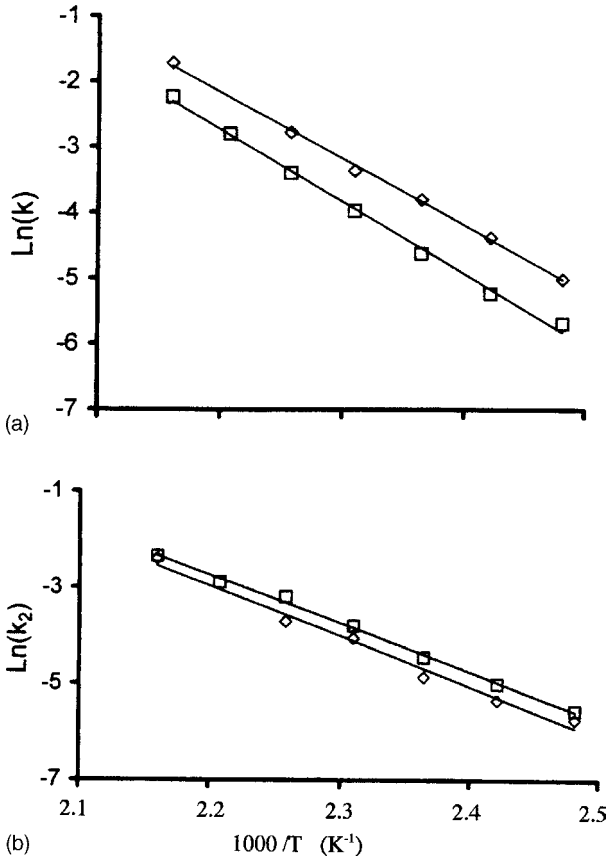

Fig. 6. Dependence of the rate of reaction on curing temperature in the two kinetic regions:(a) Plot of $\ln k$ (Eq. (11a)) and of (b) $\ln k_2$ (Eq. (11b)) as a function of 1/curing temperature.

(Fig. 6a) from which slope we obtain $E_a = 84.0\,\mathrm{kJ\,mol^{-1}}$, $A = 5.2 \times 10^8\,\mathrm{min^{-1}}$ in air and $E_a = 92.7\,\mathrm{kJ\,mol^{-1}}$, $A = 1.7 \times 10^9\,\mathrm{min^{-1}}$ in argon, in good agreement with the kinetics of catalysed cyanate resins [2,4,40,41].

The onset of diffusion control, α_d, has been obtained by locating the point where the experimental data starts to deviate from Eq. (11a). Kinetic data at $\alpha = \alpha_d$ were fitted with Eq. (11b). The average kinetic exponent, m, was 0.61 in air and 0.72 in argon. The rate constants yield $A = 9.5 \times 10^6\,\mathrm{min^{-1}}$, $E_a = 87\,\mathrm{kJ\,mol^{-1}}$ in air and $A = 2.5 \times 10^8\,\mathrm{min^{-1}}$ $E_a = 90\,\mathrm{kJ\,mol^{-1}}$ in argon from the plot of $\ln k_d$ versus $1/T$ (Fig. 6b). The experimental conversion has been fitted with Eqs. (11a) and (11b) (solid lines in Fig. 4) showing an excellent agreement between experimental conversion and model calculation.

In general, a single curve representing T_g as a function of conversion is generated from data obtained at different cure temperatures. This unique relationship between T_g and conversion is striking because one should expect that different network structures result from the cure at different temperatures. The existence of a single relationship between T_g and α enables one to use the experimental measurement of T_g to follow the conversion of the thermosetting polymer. This is particularly important at

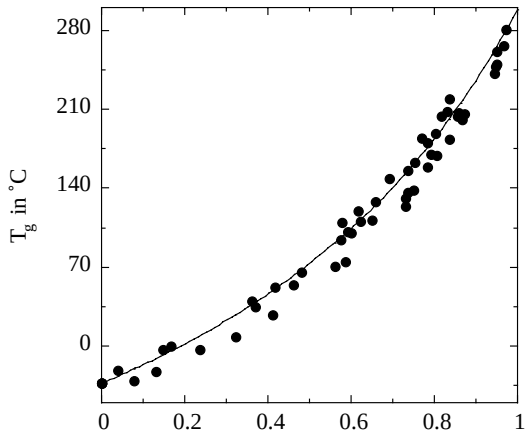

Fig. 7. Glass transition temperature as a function of conversion. The solid line is the best fit of Eq. (12) to the data.

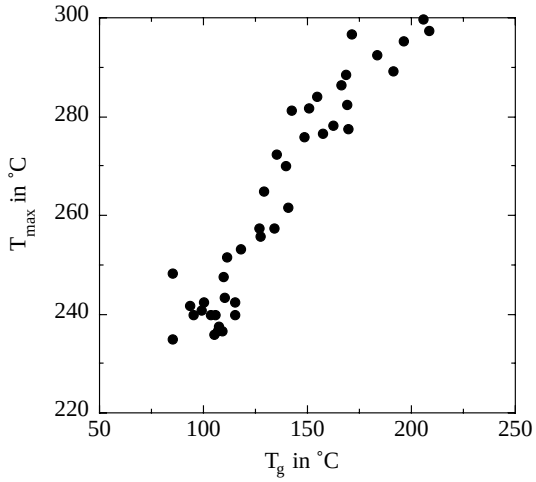

Fig. 8. Maximum exotherm temperature, T_{max}, of a dynamic scan as a function of glass transition temperature, T_g, after 4 h curing.

high conversions of the thermosetting polymer where T_g is much more sensitive to follow small increases in conversion of free functional groups than using α. The glass transition temperature of the unreacted Arocy B10, T_{g0}, is $-33\,^{\circ}C$. This temperature represents the minimum value of T_g. By rescanning a dynamically cured sample, the maximum glass transition temperature that could be attained was $T_{g\infty} = 298\,^{\circ}C$. T_g increases with curing time for the six isothermal cure temperatures because of the increase in average molecular weight and in crosslink density of the network. When T_g reaches the curing temperature the system vitrifies, and in the region where $T_g > T_c$ the glass transition temperature increases very slowly with time.

Fig. 7 depicts the glass transition temperature as a function of cyanate conversion for catalysed Arocy B10 cured at different temperatures. It is evident a one-to-one relationship between T_g and α, as usually found [7]. It is obvious for this system that there is a unique one-to-one relationship between T_g and α. Neither the curing atmosphere nor the curing temperature has a significant influence on the glass transition temperature reached by the material at a given conversion. This was expected since one assumes that there is only one product formed by the curing reaction of our cyanate ester system. Nevertheless, the curing atmosphere or/and the temperature could have a slight influence on the network structure, without significantly modifying T_g. As a consequence, the T_g can be used in our case to measure conversion. The data have been fitted with the modified DiBenedetto equation [42–44]

$$\frac{T_g - T_{g0}}{T_{g\infty} - T_{g0}} = \frac{\lambda\alpha}{1 - (1-\lambda)\alpha} \tag{12}$$

where λ is taken as an adjustable parameter, structure-dependent [45]. The plot of $(T_g - T_{g0})/(T_{g\infty} - T_{g0})$ versus α gives a value of $\lambda = 0.47$ with a master curve fitting all the experimental data indicating that the above equation is an appropriate scaling of the data. This λ value is similar to that found by Simon and Gillham (0.426) for a similar liquid resin [17], and to those reported by Pascault and Williams [45] for several epoxies networks (0.5), but higher than the obtained by Georjon et al. (0.23) for the uncatalysed system [7]. The solid line in Fig. 6 is the plot of Eq. (12).

Fig. 8 reports the maximum exotherm temperature of the residual reaction heat during a DSC scan, T_{max}, plotted as a function of the glass transition temperature for conversions higher than 0.55. It is observed an almost linear dependence between T_{max} and T_g. As conversion increases, also does T_g, the viscosity of the medium increases due to higher crosslinked matrix and the rate of reaction decreases. The reaction is no longer kinetically controlled, the rate depends on the mass transfer and it is expected to be diffusion controlled.

In order to interpret the last region of the kinetic curves, $\alpha > 0.5$–0.6, a treatment of a diffusion-affected polymerisation reaction will be investigated in the future.

4. Conclusion

The polycondensation reaction of a dicyanate ester of bisphenol A cured in the presence of cobalt(II) acetylacetonate (360 ppm) and nonylphenol (2 phr) have been investigated by differential scanning calorimetry in air and argon atmospheres. From dynamic DSC scans activation energies have been obtained. Isothermal curing reveals a higher cyanate conversion in air than in argon. Kinetic analysis shows that the experimental conversion data are fitted with a second-order kinetic equation in the kinetically controlled region, whereas an order lower than 1 has been used to fit conversion in the region of diffusion-controlled reaction. Activation energies calculated by different procedures depict a good agreement with slightly higher values in argon than in air. Glass transition temperature versus conversion shows a one-to-one relationship satisfactorily fitted with a modified DiBenedetto equation with a parameter of 0.47.

Acknowledgements

Financial support from Dirección General de Investigación (Ministerio de Ciencia y Tecnología) under Grant No. PB98-1435 is gratefully acknowledged.

References

[1] I. Hamerton, J.N. Hay, Polym. Int. 10 (1998) 163.
[2] I. Hamerton, Chemistry and Technology of Cyanate Ester Resins, Blackie Academic and Professional, Glasgow, 1994.
[3] C.P. Reghunadhan Nair, D. Mathew, K.N. Ninan, Adv. Polym. Sci. 155 (2001) 1.
[4] S.L. Simon, J. Appl. Polym. Sci. 47 (1993) 461.
[5] A. Osei-Owusu, G.C. Martin, J.T. Gotro, Polym. Eng. Sci. 31 (1991) 1604.
[6] M. Bauer, J. Bauer, G. Kühn, Acta Polym. 37 (1986) 715.
[7] O. Georjon, J. Galy, J.P. Pascault, J. Appl. Polym. Sci. 49 (1993) 1441.
[8] J. Bauer, M. Bauer, H. Much, Acta Polym. 37 (1986) 221.
[9] M. Bauer, J. Bauer, B. Garske, Acta Polym. 37 (1986) 604.
[10] Y. Deng, G.C. Martin, Polymer 37 (1996) 3593.
[11] P. Bartolomeo, J.F. Chailan, J.L. Vernet, Eur. Polym. J. 37 (2001) 659.
[12] F.B. McCormick, K.A. Brown-Wensley, R.J. Devoe, ACS 62 (1992) 460.
[13] D.A. Shimp, S.J. Ising, 35th International SAMPE Symposium, vol. 35, 1990, p. 1045.
[14] G. Van Assche, A. Van Hemelrijck, H. Rahier, B. Van Mele, Thermochim. Acta 268 (1995) 121.
[15] E. Leroy, J. Dupuy, A. Maazouz, Macromol. Chem. Phys. 202 (2001) 465.
[16] S. Vyazovkin, N. Sbirrazzuoli, Macromol. Chem. Phys. 200 (1999) 2294.
[17] S.L. Simon, J.K. Gillham, J. Appl. Polym. Sci. 47 (1993) 461.
[18] I. Harismendy, C.M. Gómez, M. Del Río, I. Mondragon, Polym. Int. 49 (2000) 735.
[19] R.H. Lin, J.L. Hong, A.C. Su, Polymer 36 (1995) 3349.
[20] M.-F. Grenier-Loustalot, C. Lartigau, F. Metras, P. Grenier, J. Polym. Sci. Part A 34 (1996) 2955.
[21] Y.-T. Chen, C.W. Macosko, J. Appl. Polym. Sci. 62 (1996) 567.
[22] Y.-H. Wang, Y.-L. Hong, J.-L. Hong, J. Appl. Polym. Sci. 58 (1995) 1585.
[23] S. Richer, S. Alamercery, F. Delolme, G. Dessalces, O. Paisse, G. Raffin, C. Sanglar, H. Waton, M.F. Grenier-Loustalot, Polym. Polym. Compos. 9 (2001) 431.
[24] O. Georjon, J. Galy, Polymer 39 (1998) 339.
[25] R.B. Prime, in: E.A. Turi (Ed.), Thermal Characterization of Polymeric Materials, Academic Press, New York, 1981 (Chapter V).
[26] J. Dupuy, E. Leroy, A. Maazouz, J.-P. Pascault, M. Raynaud, E. Bournez, Thermochim. Acta 388 (2002) 313.
[27] J.M. Barton, I. Hamerton I, J.R. Jones, Polym. Int. 31 (1993) 95.
[28] I. Harismendy, C. Gómez, M. Ormaetxea, M.D. Martin, A. Eceiza, I. Mondragon, J. Polym. Mater. 14 (1997) 317.
[29] T. Ozawa, Bull. Chem. Soc. Jpn. 38 (1965) 1881.
[30] J.M. Morancho, Ph.D. Thesis, ETSII, Barcelona (Spain), 1997.
[31] C.D. Doyle, J. Appl. Polym. Sci. 5 (1961) 285.
[32] R.B. Prime, Polym. Eng. 13 (1973) 365.
[33] S.L. Simon, J.K. Gillham, J. Appl. Sci. 46 (1992) 1245.
[34] P.A. Oyanguren, J.J. Williams, J. Appl. Polym. Sci. 47 (1993) 1361.
[35] L. Barral, J. Cano, A.J. López, J. López, P. Nogueira, C. Ramirez, Polym. Int. 38 (1995) 375.
[36] S.L. Simon, J.K. Gillham, D.A. Shimp, Proc. ACS Div. Polym. Mater. Sci. Eng. 62 (1990) 96.
[37] S.V. Vyazovkin, Int. J. Chem. Kinet. 28 (1996) 95.
[38] B.-D. Park, B. Riedl, E.W. Hsu, J. Shields, Polymer 40 (1999) 1689.
[39] J.E.K. Schawe, J. Therm. Anal. Calorim. 64 (2001) 599.
[40] A.M. Gupta, C.W. Makosko, Makromol. Chem. Macromol. Symp. 45 (1991) 105.
[41] A. Osei-Owusu, G.C. Marin, J.T. Gotro, Polym. Eng. Sci. 32 (1992) 535.
[42] J.-P. Pascault, R.J.J. Williams, J. Polym. Sci. Part B 32 (1986) 5147.
[43] L.E. Nielsen, J. Macromol. Sci., Rev. Macromol. Chem. C3 (1) (1969) 69.
[44] A.T. DiBenedetto, J. Polym. Sci. Polym. Phys. Ed. 25 (1987) 1949.
[45] J.-P. Pascault, H. Sautereau, J. Verdu, R.J.J. Williams, Thermosetting Polymers, Marcel Dekker, New York, 2002 (Chapter IV).